PROCEEDINGS, 41st Workshop on Geothermal Reservoir Engineering
Stanford University, Stanford, California, February 22-24, 2016
SGP-TR-209

Modeling the Temperature Behavior of Ground Source Heat Pump Systems

Yousef Golizadeh Akhlaghi, Omer Inanc Tureyen and Abdurrahman Satman

ITU Maden Fakultesi, Petrol ve Dogal Gaz Muh.Bol., Maslak 34469, Istanbul, TURKEY

golizadehakhla1@itu.edu.tr, inanct@itu.edu.tr, mdsatman@itu.edu.tr

Keywords: Ground source heat exchanger, modeling, underground convective flows

ABSTRACT

Ground Source Heat Exchanger Systems (GSHES) are commonplace throughout the world. Many parameters influence the behavior of GSHES. These parameters could be listed as; the thermal conductivity of the formation, the velocity of the underground water flow, the inlet temperature and etc. Mathematical models used in the modeling of GSHE performance are well established. These models usually account for the conductive heat transfer into the strata and the convective heat transfer within the tubes the fluids flow. Underground convective flows could affect the behavior of GSHES significantly. A numerical model is developed in this study for the purpose of analyzing the effects of underground water flow and various other parameters on the performance of GSHES. The model is based on solving the energy balance equation only. The energy balance considered has three main components; an accumulation term, a conductive term and a convective term. Steady state flow of fluid in the underground and in the tubes is assumed, which allows for solving only the energy balance equation. The model is verified with existing analytical and numerical solutions. The model is then used to study the effects of various parameters on the performance of GSHES.

1. INTRODUCTION

Ground sources heat exchangers have been in use since the late 1940s. The constant temperature of the earth is used as the exchange medium instead of the outside air temperature and are commonly used to either extract heat from the ground or for cooling the pre heated water for different consumptions. Various combinations exist for the geometric design of the heat exchangers. A U-tube is likely one of the most popular type of design where in this case a U-tube is located in the wellbore. Cold fluid is injected from one side of the U-tube and heated fluid is produced from the other side. In some cases two U-tubes can be used instead of one U-tube to extract heat from the underground. One of the advantages of using such an approach is that the operation can always be continued if one of the U-tubes fail. A coaxial structure could also be used where the water is injected through the loop and produced through return tube which is located in the middle of the wellbore.

The ground source heat exchanger absorbs the heat from the underground and decreases the temperature of the vicinity of the wellbore during cold fluid injection. The thermal conductivity properties of the wellbore and of the underground formation have significant effects on the amount of heat that is extracted from the earth. Normally only conduction is taken into account when modeling studies are concerned regarding the heat transfer between the wellbore and the formation. Studies exist in the literature that consider the heat transfer from the borehole into the formation by way of conduction. The early studies model the system with the line source model (Ingersoll, 1948). The temperature field for the line source solution is given by Carslaw and Jaeger (1959). The thermal response test used for estimating the thermal conductivity of the formation is given initially by Choudary (1976) and Morgensen (1983). Sanner et al. (2005) provides an overview of the Thermal Response Test. Wang et al. (2010) developed a new test method for thermal response tests. In their study a novel constant heating temperature method is used for the thermal response test. It is shown that the proposed constant heating temperature method provides shorter test times when compared with conventional thermal response tests. As a result, thermal conductivity properties of the formation can be inferred using such a methodology. Aydin et al. (2014) studied the long term performance prediction of a borehole. In their study, Aydin et al. (2014) uses an analytical model and compares them with experimental data from the lab. They also consider determining the optimal time necessary for a thermal response test. Gultekin et al. (2014) studied the optimal distance between boreholes for GSHES. They have considered various configurations of borehole spacing.

The above mentioned literature considers the heat transfer from the borehole to the formation by way of conduction only. However, in real life there may be underground water flows present. The underground water flow may affect the performance of the GSHES. This problem has been analyzed by Signorelli et al. (2007). Heterogeneity in formation properties and underground water flow have been accounted for in this study using numerical models. Akhlaghi et al. (2015) uses numerical model to study the effect of underground water flow on the performance of ground source heat exchangers.

In this study we look at the factors effecting the heat transfer in a GSHES especially in the presence of underground water flow. A very simplified numerical model that is based on steady state flow is used for this study. The model is based on solving the energy balance equation only. The energy balance equation used here includes contributions from conductive and convective transfer of heat. The model is verified with existing analytical and numerical solutions. The model is then used to study the effects of various parameters on the performance of GSHES.

2. MATHEMATICAL MODEL

In this section we review the model developed by Akhlaghi et al. (2015). The schematics of the grid blocks used in this study are given in Figure 1. The same gridding is used for the U-tube as that of the vertical gridding used in the formation. Additionally, the U-tube grids are located inside the well blocks. Energy transfer among the U-tube grids is by way of both conduction and convection. Energy transfer among the U-tube grids and the borehole grids are by way of conduction only. Energy transfer among the borehole grids and the formation grids are by way of conduction only. Finally energy transfer among the formations grids can be by way of both conduction and convection. Energy transfer by way of convection in this case will be considered in the presence of underground water movement.

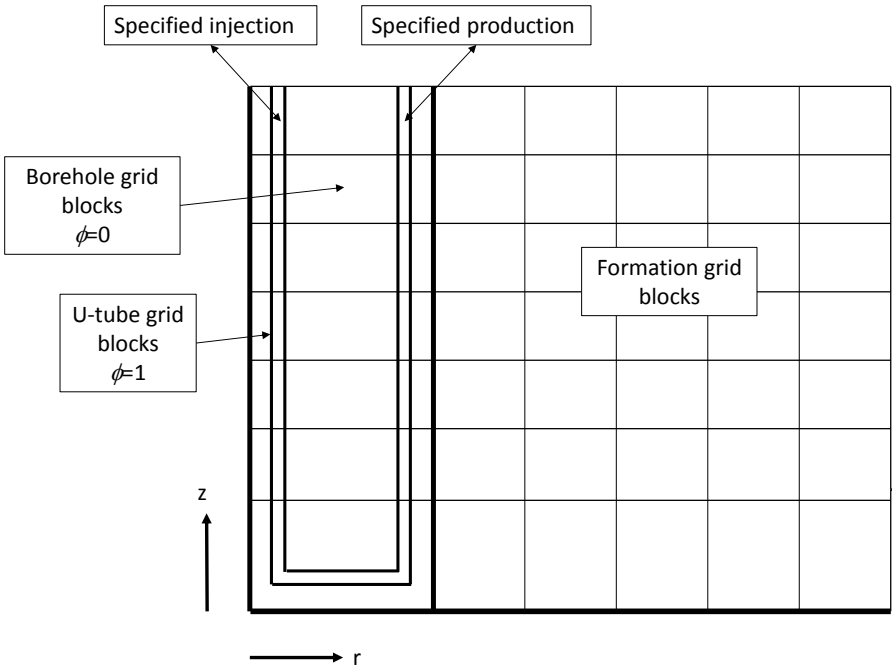

Figure 1: Schematics of the grid blocks used in the study.

As mentioned in the introduction section, in some cases there may exist two U-tubes in the borehole. The two configurations can be seen in Figure 2.

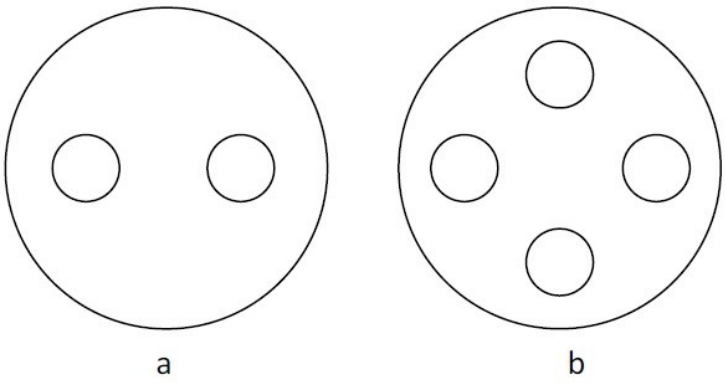

Figure 2: Various types of U-tube configurations considered in the study. a-) Borehole with one U-tube b-) Borehole with two U-tubes.

In this section the mathematical model used in this study is described. It is based on solving only the energy balance equation assuming steady state flow. The structure of the model is very similar to that developed by Tureyen and Akyapi (2011) except we do not consider the mass balance equation. Let's consider any grid *i* given in Figure 1. Figure 3 illustrates various components of heat transfer associated with grid block *i*. We presume that the grid is composed of rock and water components. Grid *i* can make an arbitrary number of connections with any other grid in the system. The total number of connections is termed *Nc*. Energy transfer by way of conduction and by way of convection is allowed for between grid *i* and the connected grids represented by j_l. The energy balance equation applied to grid *i* is given in Eq. 1.

$$\frac{d}{dt}[(1-\phi_i)V_i\rho_{m,i}C_{m,i}T_i + V_i\phi_i\rho_{w,i}u_{w,i}] + w_{inj,i}h_{w,inj,i} + w_{p,i}h_{w,i} - \sum_{l=1}^{N_{c,i}} w_{i,j_l}h_\xi - \sum_{l=1}^{N_{c,i}} \gamma_{i,j_l}(T_{j_l} - T_i) \quad (1)$$

Here V is the bulk volume (m^3), ρ is the density (kg/m^3), C is the specific heat capacity (J/kg-°C), ϕ is the porosity (fraction), T is the temperature (°C), u is the specific internal energy (J/kg), w is the mass flow rate (kg/s), h is the specific enthalpy (J/kg) and γ is the conduction index (J/°C-s). The sub indices m, w, inj and p denote the matrix, water, injection and production respectively. The first term indicates the accumulation of energy in grid i. The second term represents the energy contribution from injection, the third term indicates the energy contribution from production, the fourth term represents the energy contribution to and from neighboring grids and fifth term accounts for the contribution of energy from neighboring blocks by way of conduction.

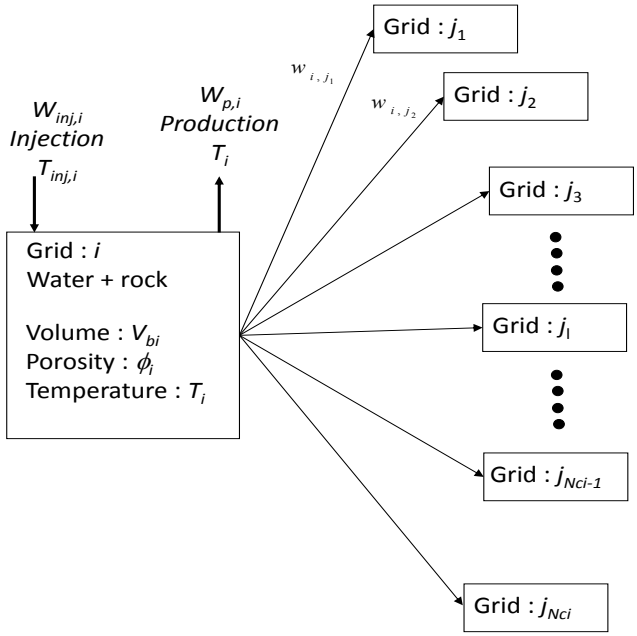

Figure 3: Illustration of any grid i and the neighboring grids.

An upwinding scheme is applied to the convective heat transfer between grid blocks. The subscript ξ denotes the direction of upwinding and is defined in Eq. 2.

$$\xi = \begin{cases} i \text{ if flow is from } i \text{ to } j_l \\ j_l \text{ if flow is from } j_l \text{ to } i \end{cases} \quad (2)$$

The conduction index can be calculated as a function of the thermal conductivity of the system. For neighboring two grid blocks in Cartesian coordinates the conduction index can be written as a function of thermal conductivity as follows:

$$\gamma_{i,j_l} = \left(\frac{\lambda A}{d}\right)_{i,j_l} \quad (3)$$

Here λ (J/m-s-°C) is the thermal conductivity of the medium, d is the distance between the grid points (m) and A is the cross sectional area between the grid blocks (m^2). It should be mentioned again that Eq. 3 is given for grid blocks that neighbor each other in the Cartesian coordinate system. The conduction index can be calculated as a function of thermal conductivity in various other coordinate systems. Harmonic averaging is applied to the thermal conductivity in determining the conduction index.

The energy balance equation is handled in a fully implicit procedure causing it to become highly non-linear. To overcome the high non-linearity a Newton Raphson method is used to solve Eq 1. Numerical derivatives used in order to create the Jacobian matrix in the Newton Raphson method. A forward difference scheme is used to handle the derivatives with respect to time.

The conduction index plays a significant role here, since energy is transferred only by way of conduction among the U-tube grids and the borehole grids. The following approximation has been made for the conduction index:

$$\gamma = \frac{\pi h \lambda r_u (r_w + r_u)}{r_o (r_o - r_u)} \tag{4}$$

Here r_u (m) is the radius of the U-tube, r_w (m) is the diameter of the borehole, h is the height of the grid. r_o (m) is given by the following relationship:

$$r_o = \frac{r_w + r_u}{2} \tag{5}$$

Eq. 4 is obtained via discretization of the diffusion equation in radial coordinates around the well. The assumption here is that the U-tube is assumed to be at the center, where as in the real case it is slightly off center as shown in Figures 1 and 2.

The conduction index between the borehole and the formation depends on the coordinate system. If a radial coordinate system is discretized, the conduction index can be determined as follows:

$$\gamma = \frac{\pi h \lambda r_w (r_b + r_w)}{r_g (r_g - r_w)} \tag{6}$$

where r_b (m) is the outer boundary radius of the grid block adjacent to the well and r_g (m) is the grid point of the same block. If discretization is carried out on Cartesian coordinates, the borehole is placed at the center of a square or a rectangle. For the conduction index between the borehole and the well, the following relation can be used:

$$\gamma = \frac{2 \pi h \lambda}{\ln \left(\frac{r_e}{r_w} \right)} \tag{7}$$

where r_e (m) can be determined as follows:

$$r_e = 0.14 \sqrt{\Delta x^2 + \Delta y^2} \tag{8}$$

where Δx (m) and Δy (m) are the lengths of the grid block bearing the borehole in the x and y directions respectively.

3. VERIFICATION

In this section we provide two cases in order to verify our numerical model. We compare our results with analytical model that is used by Aydin et al. (2014).

3.1. Analytical Model

The following dimensionless analytical equation is considered in order to verify the numerical model (Ozisik, 1993):

$$\theta (\tilde{r}, \tilde{t}) = \frac{-2}{\pi} \int_{\beta=0}^{\infty} \frac{e^{-\beta^2 \tilde{t}} [J_0(\beta \tilde{r}) Y_0(\beta) - Y_0(\beta \tilde{r}) J_0(\beta)]}{\beta (J_0^2(\beta) + Y_0^2(\beta))} d\beta \tag{9}$$

where θ is the dimensionless temperature, J is the Bessel functions of the first kind and Y is the Bessel functions of the second kind.. Dimensionless boundary and initial conditions are assumed to be:

$$\theta (1, \tilde{t}) = 0 \tag{10.1}$$

$$\theta (\tilde{r}, 0) = 1 \tag{10.2}$$

$$\theta (\infty, \tilde{t}) = 0 \tag{10.3}$$

where $\tilde{r}$ is the dimensionless radius, $\tilde{t}$ is the dimensionless time. By using the following equations dimensional boundary and initial conditions can be reached:

$$T = \theta (T_\infty - T_b) + T_b \tag{11.1}$$

$$r = \tilde{r} r_b \tag{11.2}$$

$$t = \frac{\tilde{t} r_b^2}{\alpha} \tag{11.3}$$

Here T_∞ is initial temperature of the formation, T_b is temperature of the borehole wall, r_b is radius of the borehole and α is thermal diffusivity defined by $\alpha = \lambda / \rho C$. The dimensional boundary and initial conditions are:

$$T(r_b, t) = T_b \tag{12.1}$$

$$T(r_b, 0) = T_\infty \tag{12.2}$$

$$T(\infty, t) = T_\infty \tag{12.3}$$

Table 1 gives the parameters used in the verification of the model. It is important to note that the analytical solution presented above considers a constant temperature boundary condition at the borehole. In order to mimic this effect in the developed numerical model, we assign large volumes to the borehole grid blocks during the run. This basically causes the temperature in the borehole grid blocks not to change with time, hence obtaining a constant temperature boundary condition. Furthermore the analytical model assumes a constant formation temperature. Hence in the numerical model the geothermal gradient is not used to generate the initial distribution of temperature for the verification.

Table 1: Properties of system in verification.

Initial temperature of the formation, °C	20
Temperature of borehole, °C	15
Radius of borehole, m	0.2
Thermal conductivity of formation, J/(m.s. °C)	2.92
Thermal conductivity of water in numerical study, J/(m.s. °C)	0.6
Density of rock, kg/m^3	2650
Heat capacity of formation, J/(kg. °C)	1000
Outer radius of formation, m	1000
Duration of operation, D	100
Total depth of GSHES in numerical study, m	100
Total number of grids in numerical study	256
Number of grid block in r direction in numerical study	40
Number of grid block in z direction in numerical study	5
Radius of U-tube in numerical study, m	0.02
Geothermal gradient in numerical study, °C/m	0

Figure 4 gives the temperature behavior of a specific grid point which is located at approximately 0.42 m from the borehole center. As can be seen from Figure 4, the behavior of the temperature starts from the initial value. Since the temperature behavior given in Figure 4 is the behavior at formation block, heat is transferred among the grids is only by way of conduction and the temperature starts to decrease. It is seen that the numerical profile is perfectly overlap with the analytical one.

Figure 5 gives the temperature profiles at the time of 10 Days and 100 Days. As it is clear, for both times the analytical response and the response of the numerical model overlap each other.

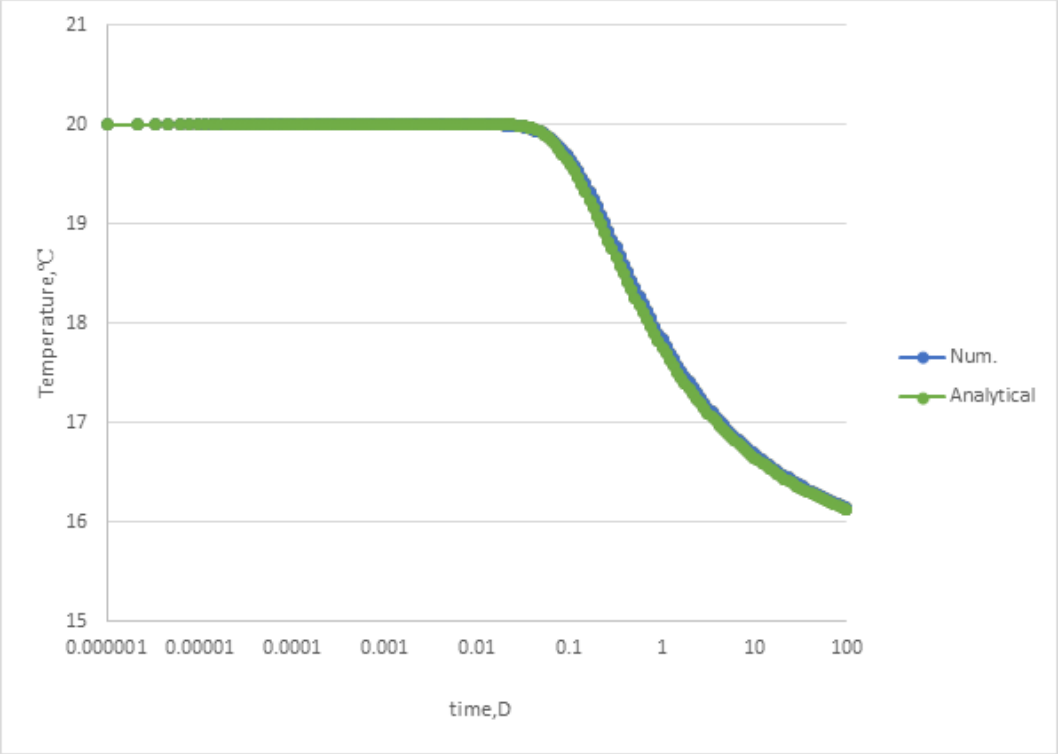

Figure 4: Comparison of the analytical model and the numerical model at 0.42 m in the formation.

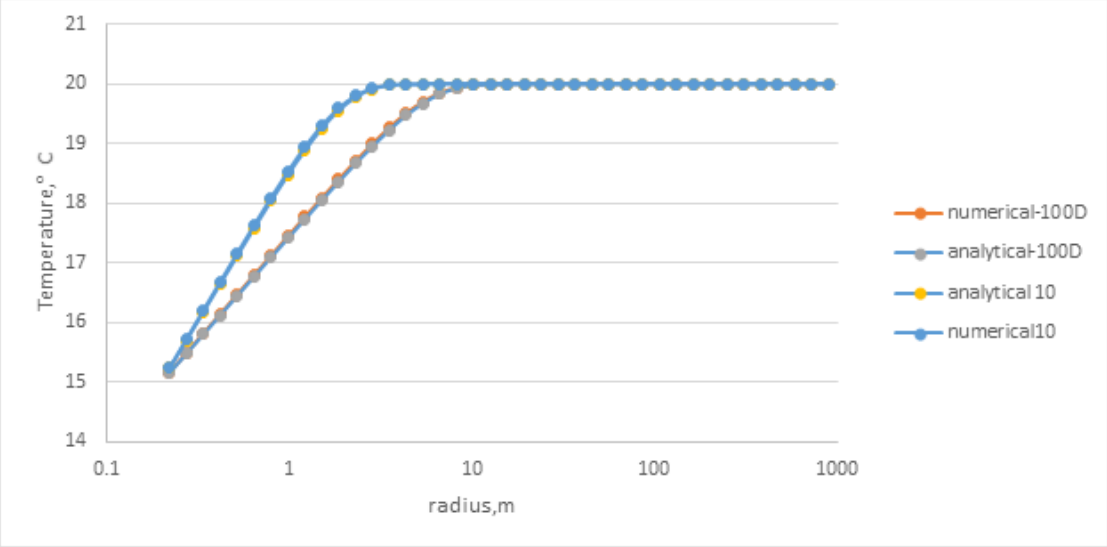

Figure 5: Comparison of the analytical model temperature distribution with the numerical model temperature distribution for 10 Days and 100Days.

4. SYNTHETIC APPLICATIONS

In this section we provide various synthetic applications to study the behavior of the GSHES. The Cartesian coordinate system will be used to investigate the effects of underground water flow on the temperature profiles of the GSHES. Additionally we use a Cartesian example to also study the effects of underground water flow rate. The properties of the formation and of the well are taken as given in Table 2 unless otherwise stated.

Table 2: Properties of system in this study.

Surface temperature, ºC	20
Radius of borehole, m	0.2
Radius of u-tube, m	0.02
Injection temperature, ºC	5
Thermal conductivity of formation, J/(m.s.ºC)	2.92
Thermal conductivity of water, J/(m.s.ºC)	0.6
Density of ground, kg/m^3	2600
Heat capacity of formation, J/(kg.ºC)	1000
Duration of operation, D	100
Total depth of GSHES, m	100
Porosity, fraction	0.1
Total number of grids	620
Radius of u-tube, m	0.02
Geothermal gradient, ºC/m	0.033

The number of grid blocks used in this study are 11×11×5. The areal grid used for this study is given in Figure 6. A logarithmic grid has been used to minimize the discretization errors around the borehole. The borehole is situated at the center of the field. Underground water flow is assumed to take place only in the fourth layer from the top. Hence the initial temperature of the fourth layer is assumed as 15 °C. Temperature of the other layers are applied by considering the geothermal gradient.

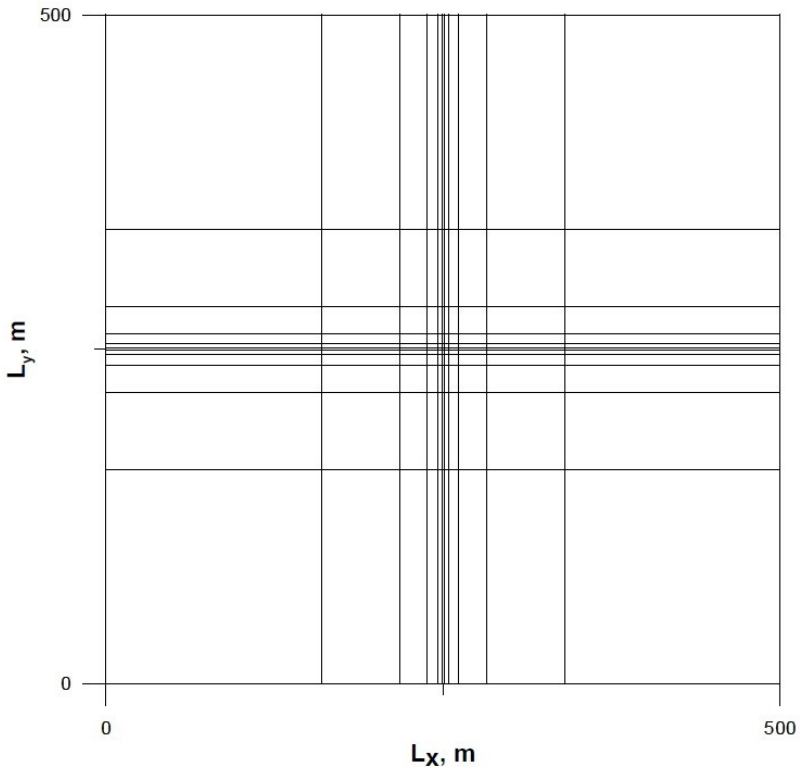

Figure 6: Areal logarithmic grid.

For analyzing the effects of underground water flow the temperature profiles around the well at 100 days are compared. Figure 7 gives the results for three various underground water flow rates. When there is no underground water flow, the profile turns out to be symmetric as expected. In this case, conduction becomes the only way of heat transfer. With an increase in the underground water flow rate, the symmetry is destroyed. At the well block, the temperature is cooled less because underground water flow serves to replenish the heat that is lost to the circulating water in the U-tube. As the water is moving from left to right, the flowing water is also cooled due to the circulating water, hence this causes the temperature profiles on the right to be smeared, extending the region where temperature changes are observed. On the left side of the well we observe the exact opposite behavior. The region of changed temperature is brought closer to the well because of the heat support from the underground water movement.

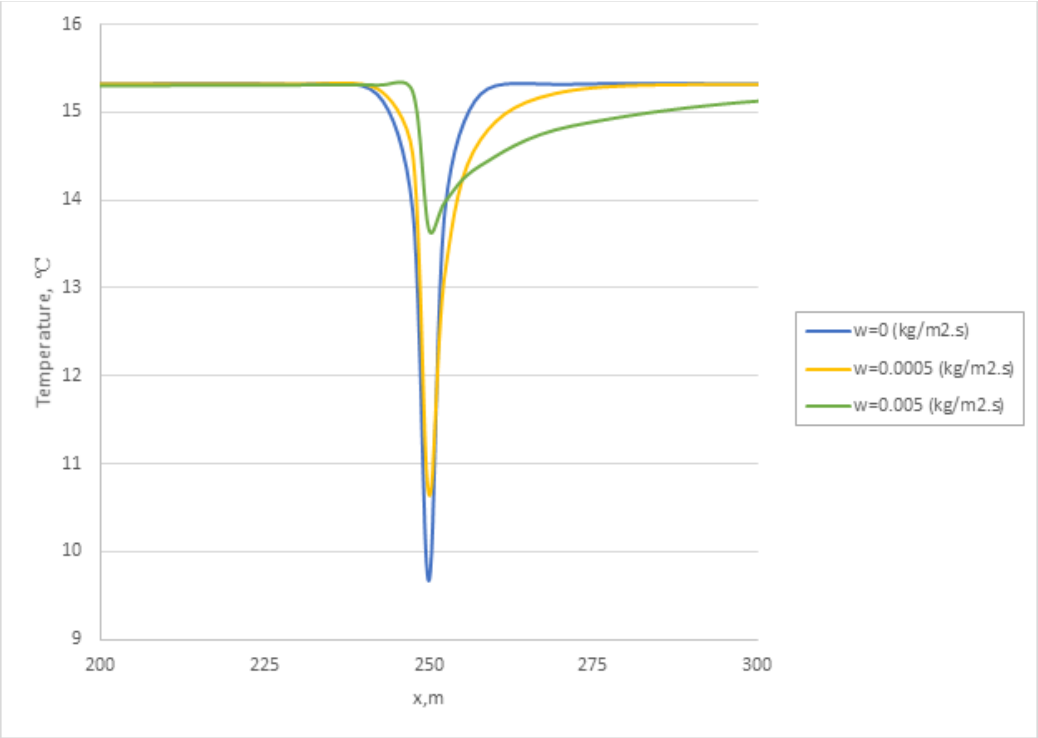

Figure 7: Temperature profiles around the well for various underground water flux.

Figure 8 gives the temperature profiles of the forth layer around the well at various days. Underground water flow is assumed to be 0.005 kg/s.m^2. In this case by increasing the time, as the water is moving from left to right, the temperature is cooled due to the circulating water in the U-tube. Again the cooling takes place on the right side of the borehole and almost no cooling is observed on the left side due to the underground water flow. The overall increase in the temperatures of the blocks are caused by conductive heat transfer between the layers. This is due to the fact that a natural state modeling has not been considered for this example and hence the temperatures change slightly away from the borehole.

Figure 9 gives the temperature behavior of the formation grids during the operation in the color-map. The same behavior for the forth layer where the underground water flow is present can be seen.

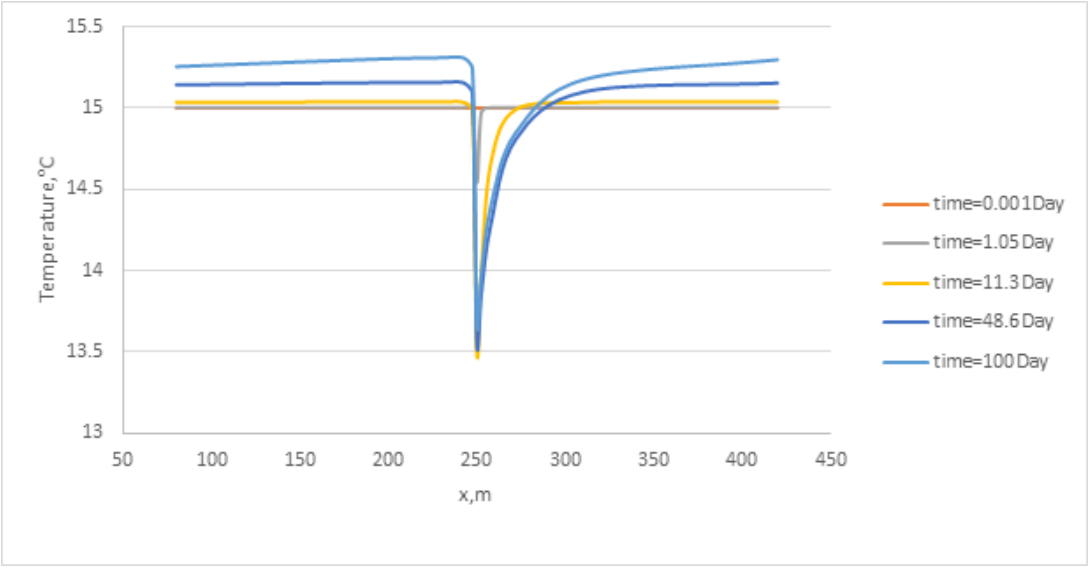

Figure 8: Temperature profiles around the well at various days.

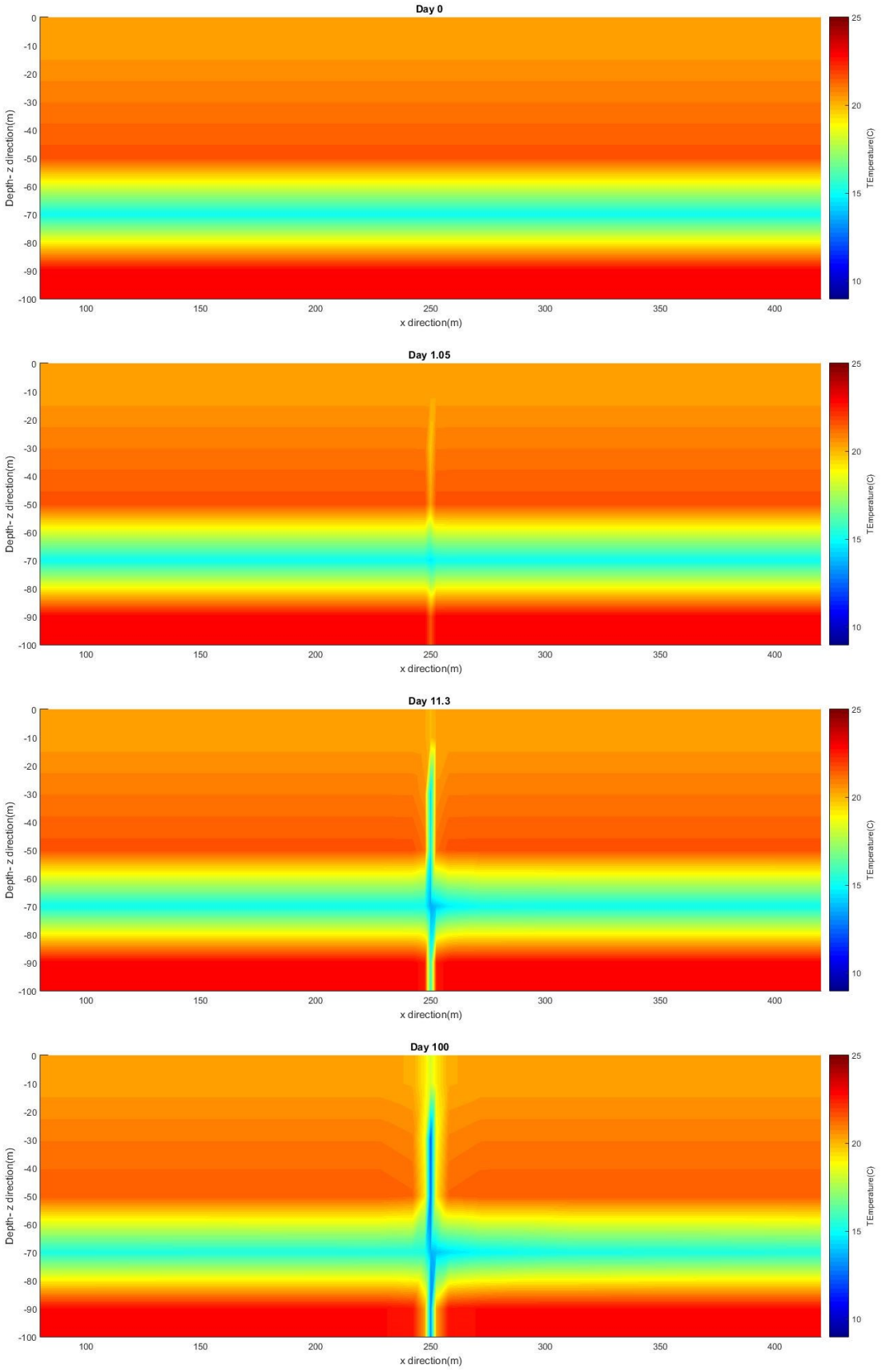

Figure 9: Temperature profiles around the well at various days.

In the final example we consider the effect of thermal conductivity on the performance of GSHES. For this purpose, three different values of the thermal conductivity are used; 1, 2.92 and 4 J/(m-s-°C). The results are given for 10 days and 100 days in Figures 10 and 11 respectively. As it is clear from Figure 11, when the thermal conductivity is low, the borehole is cooled the most since there is little heat transfer when compared with higher cases of thermal conductivity. As the thermal conductivity is increased, the well is cooled less due to higher heat transfer with the formation.

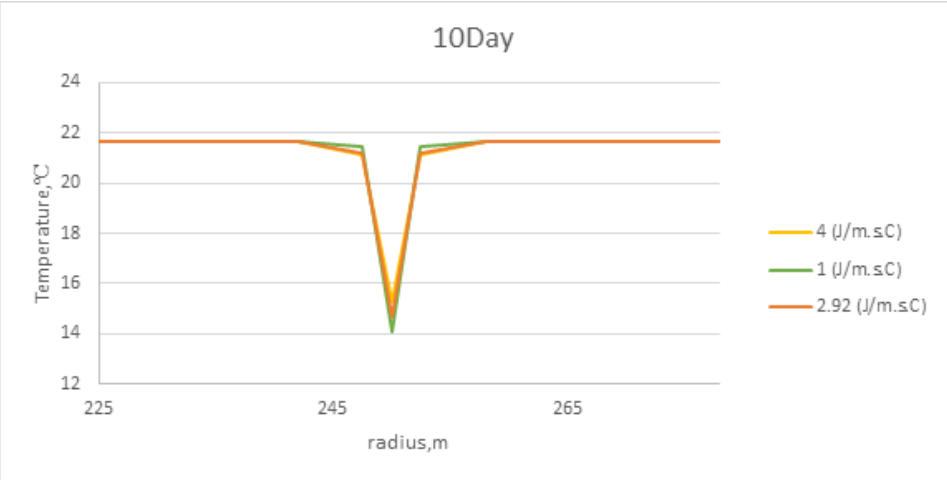

Figure 10: The temperature distribution for different formation thermal conductivities at 10 days..

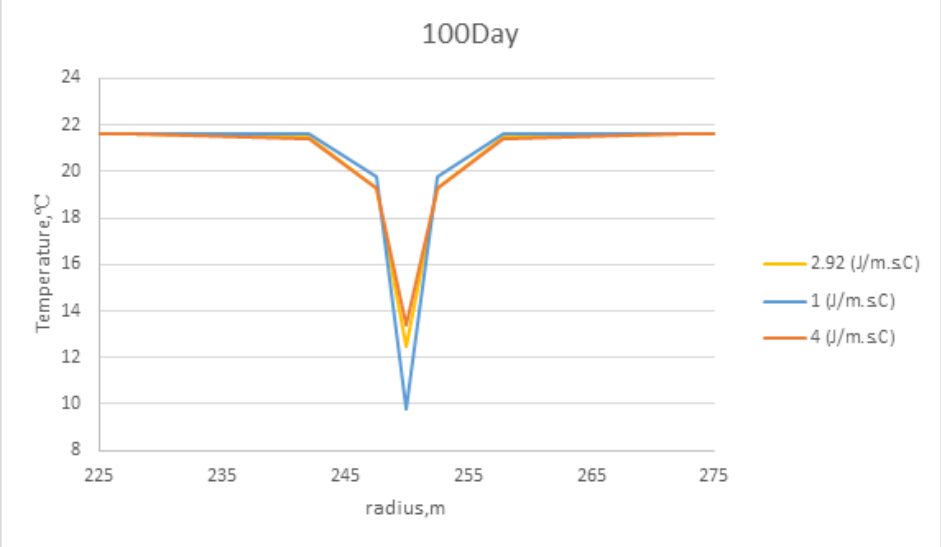

Figure 11: The temperature distribution for different formation thermal conductivities at 100 days..

5. CONCLUSIONS

The following conclusions have been obtained from this study:

- A very simple numerical model based only on solving the energy balance equation under steady state flow assumptions has been developed for modeling GSHES.
- The model has been verified with an existing analytical expression given in the literature.
- Underground water flow effects the performance of the GSHES. Higher underground water flow rates significantly affect how the temperature is distributed in the formation.
- The thermal conductivity of the formation is one of the critical factors that determine the performance of the GSHES. Lower thermal conductivities lead to more cooling due to lower heat transfer between the borehole and the formation.

REFERENCES

Akhlagi, Y. G., Kutun, K., Tureyen, O. I., and Satman, A.: (2015): Effect of Underground Convective Flows on the Performance of Ground Source Heat Exchanger Systems, *Proceedings,* 40th Workshop on Geothermal Reservoir Engineering, Stanford University, Stanford, CA.

Aydin, M., Sisman, A., and Gultekin, A. (2014): Long Term Performance Prediction of a Borehole and Determination of Optimal Thermal Response Test Duration, *Proceedings,* 39th Workshop on Geothermal Reservoir Engineering, Stanford University, Stanford, CA.

Carslaw, H. S., and Jaeger, J. C. (1959): Conduction of Heat in Solids, second ed., Oxford University Press, Oxford, UK, 510 pp.,

Choudary, A. (1976): An Approach to Determine the thermal Conductivity and Diffusivity of a Rock In Situ, *PhD Thesis,* OSU, OK.

Gultekin, A., Aydin, M., and Sisman, A. (2014): Determination of Optimal Distance Between Boreholes, *Proceedings,* 39th Workshop on Geothermal Reservoir Engineering, Stanford University, Stanford, CA.

Ingersoll, L. R., Plass, H. J. (1948): Theory of the Ground Pipe Heat Response test Evaluation, *ASHRAE Trans*, **109**, 1 – 12

Morgensen, P. (1983): Fluid to Duct Wall Heat Transfer in Duct System Heat Storage, *Proceedings,* International Conference on Surface Heat Storage in Theory and Practice, Stockholm, Sweden pp. 652 - 657.

Ozisik, N. (1993): Heat Conduction, *John Wiley & Sons Inc*.

Sanner, B., Hellstrom, G., Spitler, J., and Gehlin, S. (2005): Thermal Response Test – Current Status and World – Wide Applications, *Proceedings,* World Geothermal Congress, Antalya, TURKEY.

Signorelli, S., Basetti, S., Pahud, D., and Kohl, T. (2007): Numerical Evaluation of Thermal Response Tests, *Geothermics*, **36**, 141-166.

Tureyen, O.I., and Akyapi, E. (2011): A Generalized Non-Isothermal Tank Model for Liquid Dominated Geothermal Reservoirs, *Geothermics*, **40**, 50-57.

Verdoya, M., Imitazione, G., Chiozzi, P., Orsi, M., Armadillo, E and Pasqua, C. (2015): Interpretation of Thermal Response Tests in Borehole Heat Exchangers Affected by Advestion, *Proceedings,* World Geothermal Congress, Melbourne, AUSTRALIA.

Wang, H., Qi, C., Du, H., and Gu, Jihao. (2010): Improved Method and Case Study of Thermal Response Test for Borehole Heat Exchangers of Ground Source Heat Pump System, *Renewable Energy*, **35**, 727-733.